PHYSICAL REVIEW B **78**, 220404(R) (2008)

Optical evidence of mixed-phase behavior in manganite films

P. Gao,[1] T. A. Tyson,[1] Z. Liu,[2] M. A. DeLeon,[1] and C. Dubourdieu[3]
[1]*Department of Physics, New Jersey Institute of Technology, Newark, New Jersey 07102, USA*
[2]*Geophysical Laboratory, Carnegie Institution of Washington, Washington, DC 20015, USA*
[3]*Laboratoire des Matériaux et du Génie Physique, CNRS, Grenoble INP, 3 Parvis Louis Néel, BP 257, 38016 Grenoble, France*
(Received 25 September 2008; published 17 December 2008)

Synchrotron infrared measurements were conducted on a self-doped $La_xMnO_{3-\delta}$ ($x\sim0.8$) film. From these measurements we determined the conductivity and the temperature dependence of the effective number of carriers. While the metal-insulator transition temperature (T_{MI}) and the magnetic ordering temperature (T_C) approximately coincide, the onset of the change in the free carrier density occurs at a significantly lower temperature ($\sim$45 K below). This suggests that local distortions exist below T_{MI} and T_C which trap the e_g conduction electrons. These regions with local distortions constitute an insulating phase which persists for temperatures significantly below T_{MI} and T_C.

DOI: 10.1103/PhysRevB.78.220404 PACS number(s): 75.47.Lx, 78.20.Ls, 64.75.St, 72.80.−r

$R_{1-x}A_xMnO_3$ (R: trivalent rare-earth ions; A: divalent alkaline-earth ions) has been widely studied due to the colossal magnetoresistance (CMR) observed.[1–6] Divalent cation doping induces a change from Mn^{3+} to Mn^{4+}. The induced holes in the e_g level create a mixed-valence system. These materials have also attracted much theoretical and fundamental physics interest since they exhibit intimate coupling of spin, lattice, orbital, and charge degrees of freedom. This coupling results in a ground-state energy landscape with multiple minima corresponding to different charge, spin, and structural configurations. Small external perturbations (such as temperature, pressure, substrate strain, magnetic fields, and electric fields) can shift the system from one state to another. A mixed valence on Mn sites can also be induced in the La-deficient $La_{1-x}MnO_{3-\delta}$ ($x>0, \delta>0$) manganite. Both ferromagnetic order and metallic conductivity can be obtained,[7–9] and the transition temperatures can be adjusted by both the oxygen content and the La deficiency.[10,11] One of the open questions about these colossal magnetoresistive oxides concerns the transition of the system from the high-temperature paramagnetic insulating phase (with Jahn-Teller distortion of the MnO_6 polyhedra which trap the conduction-band electrons) to the low-temperature conductive ferromagnetic phase.[12,13] It is thought that just above the metal to insulator transition, regions of metallic phase (Jahn-Teller free) begin to grow within the insulating host and then dominate at low temperature based on structural and optical-mode measurements.[14,15] The nature of this mixed-phase behavior is still under discussion.

Optical experiments are a good way to study the phonon modes and electron-phonon coupling in oxides.[16] In addition, information on the free-carrier concentration can be derived. In previous work, it was found that the onset of the increase in the carrier numbers occurs concomitantly with the peak in resistivity and the onset of the ordered magnetic state.[17–28] In this work, we report on a synchrotron infrared spectroscopic study on self-doped $La_xMnO_{3-\delta}$ ($x\sim0.8$) films. While the metal-insulator transition temperature (T_{MI}) and the magnetic ordering temperature (T_C) approximately coincide, the change in free-carrier density onset at a significantly lower temperature ($\sim$45 K below). This indicates the presence of an insulating phase significantly below the magnetic ordering temperature.

$La_{0.8}MnO_{3-\delta}$ films were epitaxially grown on (001) $LaAlO_3$ (LAO) substrates by liquid injection metal organic chemical vapor deposition.[10] Here we report the results for a $\sim$120-nm-thick film which were also found in a $\sim$410 nm film. The *in situ* postdeposition annealing leads to the strain relaxation, and it is revealed by x-ray diffraction measurement.[29] The film resistivity is 4.6×10^{-4} Ω cm (10 K) acquired by a four-point probe setup, which is comparable with 2×10^{-4} Ω cm (5 K) for $La_{1-x}Ca_xMnO_3$ ($x=0.33$) films on a LAO substrate.[30] The metal-insulator phase-transition temperature ($T_{MI}\sim298$ K) and the Curie temperature ($T_C\sim295$ K) are quite close (see Fig. 3) and a high magnetization saturation of 3.66 μ_B/Mn (5 K) is achieved under a 0.2 T magnetic field. We have defined T_{MI} and T_C to be onset parameters corresponding to the peak in resistivity[31] and the onset of the magnetization, respectively.

Synchrotron reflectivity spectra were measured at the U2A beamline at the National Synchrotron Light Source, Brookhaven National Laboratory. This beamline has a Bruker IFS 66v/S vacuum spectrometer equipped with a Bruker IRscope-II microscope, a mercury cadmium telluride detector, and a KBr beamsplitter for mid-IR; a custom made infrared microscope with long working distant (40 mm) reflecting objective; a 3.5 micron mylar beamsplitter; and a Si bolometer detector for far-IR. The infrared frequency range covers 100–8000 cm^{-1} with a spectral resolution of 4 cm^{-1}. A $\sim$0.5-μm-thick gold layer was deposited on the film as a reflective reference mirror. The sample was mounted on the cold finger of a continuous flow cryostat, and the measurement temperatures were 304 (beginning), 282, 275, 265, 255, 245, 225, 200, 150, 125, 100, 80, 50, 20, and 10 K, which included the metal-insulator transition region.

The reflectivity spectra for the film and the bare substrate are given in Figs. 1(a) and 1(b), respectively. The vertical dashed lines correspond to phonon modes seen in other manganites.[32,33] Note the systematic enhancement of the reflectivity with decreasing temperature. Small spectral variations in the insulating LAO substrate at different temperatures can be seen in Fig. 1(b). In Fig. 1(a) the spectra (304, 282, and 275 K) show prominent LAO-like resonances in the frequency range 100–550 cm^{-1} and small differences are found in the region above 550 cm^{-1}.

More detailed information can be obtained from the re-

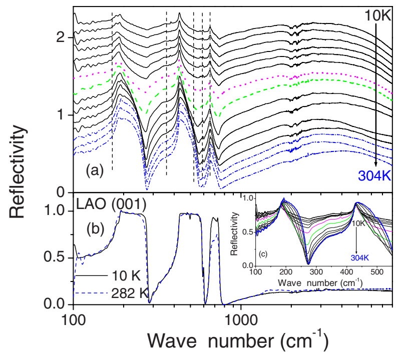

FIG. 1. (Color online) (a) $La_{0.8}MnO_{3-\delta}$/LAO reflectivity spectra at 10, 20, 50, 80, 100, 125, 150 (purple dotted lines), 200 (green dashed lines), 225, 245, 255, 265, 275 (dash dotted lines), 282 (dash dotted lines), and 304 (dash dotted lines) K on a logarithmic energy scale. The vertical dashed lines indicate phonon positions. The y scale corresponds to the 304 K spectrum, and the others are shifted up by 0.1 relative to the previous temperatures. (b) LAO substrate reflectivity spectra. The energy is given on a logarithmic scale in (a) and (b). (c) Inset is an expansion of curves in (a) over the range from 100 to 550 cm^{-1} on a linear energy scale.

flectivity spectra on an expanded scale (100–550 cm^{-1}) in Fig. 1(c). As the temperature decreases (between 275 and 200 K), the film resistance drops and the film becomes more reflective. Free carriers screen the substrate, and as a result the broad peaks at ~200 and ~450 cm^{-1} become narrow and the reflectivity drops. In the $La_{1-x}Ca_xMnO_3$ and $La_{1-x}Sr_xMnO_3$ film substrate systems and bulk samples, this phenomenon is not so obvious.[21,22,34] This phenomenon suggests incomplete conversion to the metallic phase over this temperature range. On the other hand, between 150 and 10 K, the reflectivity increases gradually in the whole frequency range except around the peaks at ~200 and ~450 cm^{-1}, as expected. A saturation level is approached below 200 K.

As the penetration depth[35] is of the order of the film thickness, the reflection from the substrate cannot be ignored especially at a low-frequency range. The reflectivity depends on the film and the substrate dielectric constants and the film thickness, after treating a one-side polished LAO substrate (0.5 mm thick) as a half-infinite plate. The dielectric functions can be described by the Drude-Lorentz (D-L) model:[35] $\varepsilon(\omega)=\varepsilon_\infty-\frac{\omega_p^2}{\omega(\omega+i\Gamma)}+\sum_j\frac{\omega_{pj}^2}{(\omega_{oj}^2-\omega^2)-i\omega\Gamma_j}$. Using the available LAO dielectric functions[36] as the initial condition, we obtain the bare substrate dielectric constant by least-squares fitting.[37] Then fixing the substrate parameters, we fit the reflectivity spectra at each temperature. An example fit at 10 K is shown in Fig. 2(a), and fitting parameters at representative temperatures are listed in Table I. The parameters (ω_{o0}, ω_{p0}, and Γ_0) correspond to the Drude contribution which yield results similar to that found previously,[20] while the second to the sixth components correspond to phonons (matching previous results). The frequencies less than 700 cm^{-1} are phonon resonances: ~170 cm^{-1} (external mode), ~350 cm^{-1} (bending mode), ~630 cm^{-1} (stretching mode), and ~520 and ~580 cm^{-1} (the oxygen vibrations).[32,33,38] Frequencies higher than 700 cm^{-1} model the effect of the polaron and band excitations.[32,33]

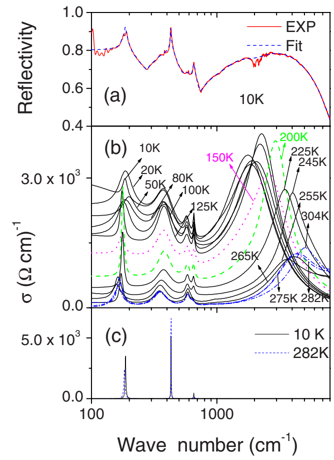

FIG. 2. (Color online) (a) An example fit of $La_{0.8}MnO_{3-\delta}$/LAO reflectivity spectra at 10 K. (b) Real part of the optical conductivity spectra of $La_{0.8}MnO_{3-\delta}$ at different temperatures. (c) Real part of the optical conductivity spectra of LAO substrate.

The optical conductivity $[\sigma(\omega)]$ can be obtained from the dielectric function: $\sigma(\omega)=-\frac{i\omega\varepsilon(\omega)}{4\pi}$. Temperature-dependent $\sigma(\omega)$ are plotted for the film [Fig. 2(b)] and the substrate [Fig. 2(c)]. The spectral weight of the Drude components of the film increases as the temperature decreases and the peak above 1000 cm^{-1} which like a small polaron feature moves toward the low-frequency side with decreasing temperature (as has been discussed in detail in Refs. 34 and 39). The peak maximum shifts from ~5100 cm^{-1} at 304 K to ~4300 cm^{-1} at 282 K. The polaron shifts to the low-energy side quickly and below 255 K the spectral weight increases dramatically as the carrier mobility increases with reduced temperature. Below 200 K, the reflectivity spectra and the optical spectra vary slowly with the temperature. Figure 2(c) shows LAO substrate optical spectra at two different temperatures. The positions do not change significantly with temperature (<4 cm^{-1}) while the amplitudes vary.

In addition, the zero-frequency conductivity, plasma frequency (ω_p), and resistivity are related by $\sigma(0)=\frac{ne^2\tau}{m}$, $\omega_p^2=\frac{4\pi ne^2}{m}$, and $\rho=\frac{1}{4\pi\omega_p^2\tau}$. We plotted the dc resistivity and calculated resistivity [from $\sigma(0)$] in Fig. 3(a) with the magnetization. The resistivity data sets have a consistent trend and

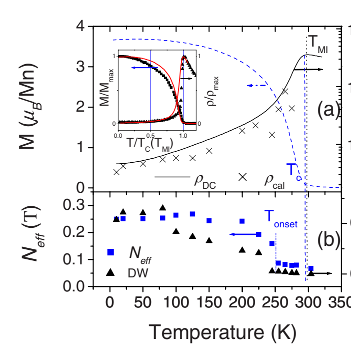

FIG. 3. (Color online) (a) Magnetization and calculated and measured dc resistivities of $La_{0.8}MnO_{3-\delta}$/LAO film. Inset is the comparison for $La_{2/3}Ca_{1/3}MnO_3$ (symbols) and $La_{0.8}MnO_{3-\delta}$ (line). (b) Effective carrier numbers and Drude weight (free carriers).

TABLE I. D-L model fitting parameters at 304, 282, 275, 265, 150, 125, and 10 K. Note: ω_o, ω_P, and Γ in unit cm^{-1}.

	304 (K)	282 (K)	275 (K)	265 (K)	150 (K)	125 (K)	10 (K)
ε_∞	5.2	5.6	5.5	5.5	5.5	5.5	5.5
ω_{o0}		0	0	0	0	0	0
ω_{p0}		1016	1184	1508	6413	6782	8142
Γ_0		17	98	314	531	442	366
ω_{o1}	167	162	167	168	173	175	185
ω_{p1}	1039	925	826	718	760	950	769
Γ_1	34	33	18	18	23	13	21
ω_{o2}	356	350	350	350	378	381	382
ω_{p2}	1500	1515	1455	1319	2489	2941	3271
Γ_2	107	112	100	90	134	128	169
ω_{o3}	523	524	524	523	535		
ω_{p3}	311	316	383	601	726		
Γ_3	60	57	72	123	69		
ω_{o4}	584	585	585	586	585	577	575
ω_{p4}	853	897	885	888	1010	1509	1742
Γ_4	53	54	52	52	52	86	97
ω_{o5}	636	642	641	638	659	656	657
ω_{p5}	615	533	534	448	877	842	893
Γ_5	77	46	48	39	39	30	29
ω_{o6}	908	958	940	984			974
ω_{p6}	710	826	861	1029			4226
Γ_6	328	400	413	540			702
ω_{o7}	4881	4177	4304	4129	2123	1732	1899
ω_{p7}	8541	15085	15952	17064	17908	14955	19233
Γ_7	2215	3526	3822	4181	3682	3037	1988
ω_{o8}	5564	8988	9178	7795	2654	2318	
ω_{p8}	19684	17922	17315	6794	13366	15866	
Γ_8	7416	9101	8447	2729	1763	1474	

show good agreement for temperatures where the sample is more metallic, indicating that the D-L model is appropriate. Figure 3(a) inset shows that the deficient $La_{0.8}MnO_{3-\delta}$ is a normal CMR material in terms of the widths of the transition regions (for magnetization and resistivity) compared with $La_{2/3}Ca_{1/3}MnO_3$ film.[31] Note the similarity in widths in the magnetization and resistivity transition regions.

The effective carrier number density $N_{\rm eff}(T,\omega_c)$ is proportional to the integrated optical conductivity spectral weight: $N_{\rm eff}(T,\omega_c)=\frac{2mV}{\pi e^2}\int_0^{\omega_c}\mathrm{Re}\,\sigma(\omega')d\omega'$. We use a cutoff frequency (ω_c) of 5000 cm^{-1} to calculate the number density ($N_{\rm eff}$). $N_{\rm eff}(T)$ and Drude weight (DW) (the $N_{\rm eff}$ of free carriers only) are plotted in Fig. 3(b) (see Ref. 20). By examining the cutoff frequency dependence of the shape of $N_{\rm eff}$ vs temperature in the broad set of manganite data in Refs. 35 and 40, we found that the onset profile is independent of ω_c for cutoff frequencies ranging from 4800 to 32 000 cm^{-1}. Moreover the onset temperature found is insensitive to the choice of ε_∞ over a physically meaningful range. It can be seen that the onset of the increase in $N_{\rm eff}$(~253 K) is significantly below $T_{\rm MI}$ and T_C. The free-carrier Drude weight is small compared with the $N_{\rm eff}$, and its onset occurs at ~245 K. The results indicate that the increase in carrier concentration lags the onset of magnetic order by ~45 K.

The results suggest a more complex mechanism for the transition to the low-temperature phase in manganites. It is consistent with the existence of regions with significant local distortions below $T_{\rm MI}$ and T_C which trap the e_g conduction electrons. These regions with local distortions constitute an insulating phase which persists for temperatures significantly below $T_{\rm MI}$ and T_C. Low spin scattering will lead to the observed initial large resistivity drop[41] as a result of magnetic ordering of the t_{2g} spins enabling Mn-Mn site hopping[42,43] when reducing temperature below T_C. Further reductions in resistivity are then due to reductions in the volume of the minority insulating phase which then increases the number of free carriers. The origin of the flattening of the reflectivity spectra at low temperature is due to the increased number of free carriers, which limits the penetration depth of the light into the sample.

In conclusion, we have explored the temperature-dependent infrared reflectivity spectra of $La_xMnO_{3-\delta}$/LAO

($x \sim 0.8$) system over the range 100–8000 cm^{-1}. While the metal-insulator transition temperature (T_{MI}) and the magnetic ordering temperature (T_C) approximately coincide, the free-carrier density onset occurs at a significantly lowered temperature (~45 K below). The conductivity was found to be systematically enhanced at lower temperatures. These results are consistent with the existence of insulating regions at temperatures significantly below the metal-insulator and magnetic ordering temperatures.

This research was funded by NSF (Grants No. DMR-0512196 and No. INT-0233316) and CNRS/NSF (Project No. 14550). U2A beamline is supported by COMPRES, the Consortium for Materials Properties Research in Earth Sciences under NSF Cooperative Agreement No. EAR01-35554 and U.S. Department of Energy (DOE-BES and NNSA/CDAC). Use of the National Synchrotron Light Source, Brookhaven National Laboratory was supported by the Office of Science, Office of Basic Energy Sciences, U.S. Department of Energy under Contract No. DE-AC02-98CH10886.

[1] S. Jin, T. H. Tiefel, M. McCormack, R. A. Fastnacht, R. Ramesh, and L. H. Chen, Science **264**, 413 (1994).
[2] C. N. R. Rao, A. K. Cheetham, and R. Mahesh, Chem. Mater. **8**, 2421 (1996).
[3] M. B. Salamon and M. Jaime, Rev. Mod. Phys. **73**, 583 (2001).
[4] J. M. D. Coey, M. Viret, and S. Von Molnar, Adv. Phys. **48**, 167 (1999).
[5] *Colossal Magnetoresistive Oxides*, edited by Y. Tokura (Gordon and Breach Science, London, 1999).
[6] W. Prellier, Ph Lecoeur, and B. Mercey, J. Phys.: Condens. Matter **13**, R915 (2001).
[7] J. Topfer and J. B. Goodenough, Chem. Mater. **9**, 1467 (1997).
[8] A. Maignan, C. Michel, M. Hervieu, and B. Raveau, Solid State Commun. **101**, 277 (1997).
[9] A. A. Bosak, O. Yu Gorbenko, A. R. Kaul, I. E. Graboy, C. Dubourdieu, J. P. Senateur, and H. W. Zandbergen, J. Magn. Magn. Mater. **211**, 61 (2000).
[10] A. Bosak, C. Dubourdieu, M. Audier, J. P. Sénateur, and J. Pierre, Appl. Phys. A **79**, 1979 (2004).
[11] Z. Chen, T. A. Tyson, K. H. Ahn, Z. Zhong, and J. Hu, arXiv:0708.1963.
[12] A. Moreo, S. Yunoki, and E. Dagotto, Science **283**, 2034 (1999).
[13] K. H. Ahn, T. Lookman, and A. R. Bishop, Nature (London) **428**, 401 (2004).
[14] S. J. L. Billinge, T. Proffen, V. Petkov, J. L. Sarrao, and S. Kycia, Phys. Rev. B **62**, 1203 (2000).
[15] H. L. Liu, S. Yoon, S. L. Cooper, S. W. Cheong, P. D. Han, and D. A. Payne, Phys. Rev. B **58**, R10115 (1998).
[16] F. Gervais, Mater. Sci. Eng. R. **39**, 29 (2002).
[17] Y. Okimoto, T. Katsufuji, T. Ishikawa, A. Urushibara, T. Arima, and Y. Tokura, Phys. Rev. Lett. **75**, 109 (1995).
[18] S. G. Kaplan, M. Quijada, H. D. Drew, D. B. Tanner, G. C. Xiong, R. Ramesh, C. Kwon, and T. Venkatesan, Phys. Rev. Lett. **77**, 2081 (1996).
[19] K. H. Kim, J. H. Jung, D. J. Eom, T. W. Noh, Yu. Jaejun, and E. J. Choi, Phys. Rev. Lett. **81**, 4983 (1998).
[20] K. H. Kim, J. H. Jung, and T. W. Noh, Phys. Rev. Lett. **81**, 1517 (1998).
[21] A. V. Boris, N. N. Kovaleva, A. V. Bazhenov, P. J. M. van Bentum, Th Rasing, S. W. Cheong, A. V. Samoilov, and N. C. Yeh, Phys. Rev. B **59**, R697 (1999).
[22] Y. Okimoto, T. Katsufuji, T. Ishikawa, T. Arima, and Y. Tokura, Phys. Rev. B **55**, 4206 (1997).
[23] T. Ishikawa, T. Kimura, T. Katsufuji, and Y. Tokura, Phys. Rev. B **57**, R8079 (1998).
[24] H. J. Lee, J. H. Jung, Y. S. Lee, J. S. Ahn, T. W. Noh, K. H. Kim, and S. W. Cheong, Phys. Rev. B **60**, 5251 (1999).
[25] N. Petit, C. Daulan, J. C. Soret, A. Maignan, and F. Gervais, Eur. Phys. J. B **14**, 617 (2000).
[26] A. Nucara, A. Perucchi, P. Calvani, T. Aselage, and D. Emin, Phys. Rev. B **68**, 174432 (2003).
[27] H. Okamura, T. Koretsune, M. Matsunami, S. Kimura, T. Nanba, H. Imai, Y. Shimakawa and Y. Kubo, Phys. Rev. B **64**, 180409(R) (2001).
[28] C. A. Perroni, G. De Filippis, V. Cataudella, and G. Iadonisi, Phys. Rev. B **64**, 144302 (2001).
[29] Q. Qian, T. A. Tyson, C. Dubourdieu, A. Bossak, J. P. Senateur, M. Deleon, J. Bai, G. Bonfait, and J. Maria, J. Appl. Phys. **92**, 4518 (2002).
[30] G. J. Snyder, R. Hiskes, S. DiCarolis, M. R. Beasley, and T. H. Geballe, Phys. Rev. B **53**, 14434 (1996).
[31] Ch. Hartinger, F. Mayr, A. Loidl, and T. Kopp, Phys. Rev. B **70**, 134415 (2004).
[32] H. L. Liu, M. X. Kuo, J. L. Her, K. S. Lu, S. M. Weng, L. M. Wang, S. L. Cheng, and J. G. Lin, J. Appl. Phys. **97**, 113528 (2005).
[33] H. L. Liu, K. S. Lu, M. X. Kuo, S. Uba, L. Uba, M. Wang, and H. T. Jeng, J. Appl. Phys. **99**, 043908 (2006).
[34] Ch. Hartinger, F. Mayr, A. Loidl, and T. Kopp, Phys. Rev. B **73**, 024408 (2006).
[35] F. P. Mena, A. B. Kuzmenko, A. Hadipour, J. L. M. van Mechelen, D. van der Marel, and N. A. Babushkina, Phys. Rev. B **72**, 134422 (2005).
[36] Z. M. Zhang, B. I. Choi, M. I. Flik, and A. C. Anderson, J. Opt. Soc. Am. B **11**, 2252 (1994).
[37] A. B. Kuzmenko, Rev. Sci. Instrum. **76**, 083108 (2005).
[38] I. Fedorov, J. Lorenzana, P. Dore, G. DeMarzi, P. Maselli, P. Calvani, S. W. Cheong, S. Koval, and R. Migoni, Phys. Rev. B **60**, 11875 (1999).
[39] D. Emin, Phys. Rev. B **48**, 13691 (1993).
[40] M. Quijada, J. Černe, J. R. Simpson, H. D. Drew, K. H. Ahn, A. J. Millis, R. Shreekala, R. Ramesh, M. Rajeswari, and T. Venkatesan, Phys. Rev. B **58**, 16093 (1998).
[41] Y. Lyanda-Geller, S. H. Chun, M. B. Salamon, P. M. Goldbart, P. D. Han, Y. Tomioka, A. Asamitsu, and Y. Tokura, Phys. Rev. B **63**, 184426 (2001).
[42] Y. Tomioka, H. Kuwahara, A. Asamitsu, T. Kimura, R. Kumai, and Y. Tokura, Physica B **246–247**, 135 (1998).
[43] Y. Tomioka, A. Asamitsu, H. Kuwahara, Y. Moritomo, and Y. Tokura, Phys. Rev. B **53**, R1689 (1996).